

**Resonant behavior of a fractional oscillator with fluctuating frequency**Erkki Soika,<sup>\*</sup> Romi Mankin, and Ain Ainsaar*Institute of Mathematics and Natural Sciences, Tallinn University, 25 Narva Road, 10120 Tallinn, Estonia*

(Received 21 July 2009; revised manuscript received 25 September 2009; published 29 January 2010)

The long-time behavior of the first moment for the output signal of a fractional oscillator with fluctuating frequency subjected to an external periodic force is considered. Colored fluctuations of the oscillator eigenfrequency are modeled as a dichotomous noise. The viscoelastic type friction kernel with memory is assumed as a power-law function of time. Using the Shapiro-Loginov formula, exact expressions for the response to an external periodic field and for the complex susceptibility are presented. On the basis of the exact formulas it is demonstrated that interplay of colored noise and memory can generate a variety of cooperation effects, such as multiresonances versus the driving frequency and the friction coefficient as well as stochastic resonance versus noise parameters. The necessary and sufficient conditions for the cooperation effects are also discussed. Particularly, two different critical memory exponents have been found, which mark dynamical transitions in the behavior of the system.

DOI: [10.1103/PhysRevE.81.011141](https://doi.org/10.1103/PhysRevE.81.011141)

PACS number(s): 05.40.-a, 02.50.-r, 45.10.Hj

**I. INTRODUCTION**

Noise-induced phenomena in complex systems present a fascinating subject of investigation since, contrary to all intuition, environmental randomness may induce more order in the behavior of the system. Stochastic resonance (SR) [1–3], the ratchet effect [4], noise-induced spatial patterns [5], first-order phase transitions [6], noise-induced multistability in some models of ecological systems [7,8], as well as anomalous diffusion [9], are a few examples in this field. One of the objects of special attention in this context is the noise-driven harmonic oscillator. The harmonic oscillator is the simplest toy model for different phenomena in nature and as such it is the typical theoretician's paradigm for various fundamental conceptions [10]. Since Chandrasekhar [11] originally considered the problem of noise-driven dynamics of a Brownian harmonic oscillator, the study of a harmonic oscillator with random frequency is a subject that has been extensively investigated in different fields including physics [12,13], biology [14], and chemistry [15]. In most of the previous analysis the influence of white noise is considered. However, more realistic models of many systems, e.g., biological ones require considering a colored noise [16]. It is shown that the influence of colored noise on the oscillator eigenfrequency may lead to different resonant phenomena. First, it may cause energetic instability [12,17,18]. This phenomenon is a stochastic counterpart of classical parametric resonance [12,19]. Second, for bistable oscillators driven by a periodic dichotomous noise a noise-induced coherence occurs, which manifests itself as fractal trajectory patterns in the phase plane of the Poincaré map of the flow [20]. Third, if the oscillator is subjected to an external periodic force, the behavior of the amplitude of the first moment of the output signal shows a nonmonotonic dependence on noise parameters, i.e., SR [18,21,22]. To avoid misunderstandings, let us mention that we use the term stochastic resonance in a wide sense, meaning the nonmonotonic behavior of the output sig-

nal or some function thereof (moments, signal-to-noise ratio) in response to noise parameters [3,21,23].

Another popular generalization of the harmonic oscillator consists in replacing the usual friction term in the dynamical equation for a harmonic oscillator by a generalized friction term with a power-law-type memory [24–26]. The dynamical equation for such an oscillator is a special case of the more general fractional Langevin equation (see, e.g., [27]). The main advantage of this equation is that it provides a physically transparent and mathematically tractable description of the stochastic dynamics in systems with slow relaxation processes and with anomalous slow diffusion (subdiffusion). Examples of such systems are supercooled liquids, glasses, colloidal suspensions, dense polymer solutions [28,29], viscoelastic media [30], and amorphous semiconductors [31]. Even anomalous diffusive dynamics of atoms in biological macromolecules and intrinsic conformational dynamics of proteins can be subdiffusive [26,32]. This method has also been successfully used in describing anomalous diffusion phenomena for reaction kinetics and fluorescence intermittency of single enzymes [33] and for nuclear fusion reactions [34].

Although the behavior of both above-mentioned generalizations of the harmonic oscillator are investigated in detail (see, e.g., [18,24]), it seems that proper analysis of the potential consequences of an interplay of colored eigenfrequency fluctuations, external periodic forcing, and memory effects in an oscillator is still missing in literature. This is quite surprising in view of the fact that the importance of colored fluctuations and viscoelasticity (friction with a long-time memory) for biological systems, e.g., for living cells, has been well recognized [30,35].

Thus motivated, we consider a fractional oscillator with a power-law memory kernel subjected to an external periodic force. The influence of the fluctuating environment is modeled by a multiplicative dichotomous noise (fluctuating eigenfrequency).

The main purpose of this paper is to provide exact formulas for analytical treatment of the dependence of certain output characteristics of the oscillator, such as the response function and complex susceptibility, on various system pa-

<sup>\*</sup>erkki.soika@tlu.ee

rameters: viz. the noise correlation time, noise amplitude, friction coefficient, memory exponent, and driving frequency. Based on those exact expressions we demonstrate that SR is manifested in the dependence of the output characteristics of the noisy fractional oscillator upon the noise parameters. Furthermore, we will show that in certain parameter regions the response function and the complex susceptibility of the oscillator exhibit a multiresonance behavior versus the driving frequency, and even versus the friction coefficient. Moreover, we have found two critical memory exponents  $\alpha$ , which mark the transitions between various dynamical regimes of the oscillator.

To our knowledge, some resonance phenomena considered in this paper, e.g., a multiresonancelike dependence of the amplitude of the mean oscillator displacement on the friction coefficient  $\gamma$ , a two-band structure of the  $\gamma$ - $\alpha$  phase diagrams for the existence of SR and the associated friction-induced re-entrant transitions between different dynamical regimes of the oscillator, are noise-induced effects that have never been observed, let alone discussed before.

The structure of the paper is as follows. In Sec. II we present the model investigated. Exact formulas are found for the long-time behavior of the first moment of the oscillator displacement and for the complex susceptibility. In Sec. III we analyze the dependence of the output characteristics on the system parameters. Section IV contains some brief concluding remarks. Some formulas are delegated to the Appendix.

## II. MODEL AND COMPLEX SUSCEPTIBILITY

### A. Model

As a model for an oscillatory system strongly coupled with a noisy environment, we consider a dichotomously perturbed oscillator with a power-law-type memory friction kernel

$$\begin{aligned} \ddot{X} + \frac{\gamma}{\Gamma(1-\alpha)} \int_0^t \frac{1}{(t-t')^\alpha} \dot{X}(t') dt' + [\omega^2 + Z(t)]X \\ = A_0 \cos(\Omega t), \end{aligned} \quad (1)$$

where  $\dot{X} \equiv dX/dt$ ,  $X(t)$  is the oscillator displacement,  $\gamma$  is a friction constant,  $0 < \alpha < 1$  is the fractional exponent, and  $\Gamma$  is the gamma function. Fluctuations of the frequency  $\omega^2$  are expressed by a Markovian dichotomous noise  $Z(t)$ , which consists of jumps between two values:  $z_1 = a$  and  $z_2 = -a$ , with  $a > 0$  [36]. The jumps follow, in time, the pattern of a Poisson process, the values occurring with the stationary probabilities  $p_s(a) = p_s(-a) = 1/2$ . In a stationary state the fluctuation process  $Z(t)$  satisfies

$$\langle Z(t) \rangle = 0, \quad \langle Z(t + \tau)Z(t) \rangle = a^2 e^{-\nu|\tau|}, \quad (2)$$

where the switching rate  $\nu$  is the reciprocal of the noise correlation time  $\tau_c = 1/\nu$ , i.e.,  $Z(t)$  is a symmetric zero-mean exponentially correlated noise. As in this work we will restrict ourselves to the behavior of the first moment  $\langle X(t) \rangle$ , all results are also applicable in models where an additive noise  $\xi(t)$ , which is statistically independent from  $Z(t)$  and has a

zero mean, is included on the right side of Eq. (1). For example, depending on the physical situation, the noise  $\xi(t)$  can be regarded either as an internal noise, in which case its stationary correlation satisfies Kubo's second fluctuation-dissipation theorem [37] expressed as

$$\langle \xi(t + \tau)\xi(t) \rangle = k_B T \gamma [\Gamma(1-\alpha)]^{-1} |\tau|^{-\alpha},$$

(here  $k_B$  is the Boltzmann constant and  $T$  is the temperature of the heat bath), or as an external noise, in which case the driving noise  $\xi(t)$  and the dissipation may have different origins and no fluctuation-dissipation relation holds.

To find the first moment of  $X$ , we use the well-known Shapiro-Loginov procedure [38], which for an exponentially correlated noise  $Z(t)$  yields

$$\frac{d}{dt} \langle Zm \rangle = \left\langle Z \frac{dm}{dt} \right\rangle - \nu \langle Zm \rangle, \quad (3)$$

where  $m$  is an arbitrary function of the noise,  $m = m(Z)$ .

From Eqs. (1) and (3), we thus obtain an exact linear system of four first-order integrodifferential equations for four variables,  $x_1 \equiv \langle X \rangle$ ,  $x_2 \equiv \langle \dot{X} \rangle$ ,  $x_3 \equiv \langle ZX \rangle$ , and  $x_4 \equiv \langle Z\dot{X} \rangle$ ,

$$\dot{x}_1 = x_2,$$

$$\dot{x}_2 = -\omega^2 x_1 - x_3 - \frac{\gamma}{\Gamma(1-\alpha)} \int_0^t \frac{x_2(t') dt'}{(t-t')^\alpha} + A_0 \cos(\Omega t),$$

$$\dot{x}_3 = x_4 - \nu x_3,$$

$$\begin{aligned} \dot{x}_4 = -a^2 x_1 - \omega^2 x_3 - \nu x_4 \\ - \frac{\gamma}{\Gamma(1-\alpha)} e^{-\nu t} \int_0^t \frac{x_4(t')}{(t-t')^\alpha} e^{\nu t'} dt'. \end{aligned} \quad (4)$$

The solution of Eqs. (4) can be represented in the form

$$x_i(t) = \sum_{k=1}^4 H_{ik}(t) x_k(0) + A_0 \int_0^t H_{i2}(t-t') \cos(\Omega t') dt', \quad (5)$$

where the constants of integration  $x_k(0)$  are determined by the initial conditions and the relaxation functions  $H_{ik}(t)$ , with  $H_{ik}(0) = \delta_{ik}$ , are the inverse forms of the Laplace transforms  $\hat{H}_{ik}(s)$  given by Eq. (A2) in the Appendix. One can check the stability of solution (5), which, according to the results of Ref. [39], means that, the solutions  $s_j$  of the equation [cf. Eq. (A2)]

$$(s^2 + \gamma s^\alpha + \omega^2)[(s + \nu)^2 + \gamma(s + \nu)^\alpha + \omega^2] - a^2 = 0, \quad (6)$$

cannot have roots with a positive real part. This requirement is met if the inequality

$$a^2 < a_{cr}^2 = \omega^2(\omega^2 + \gamma\nu^\alpha + \nu^2), \quad (7)$$

holds. Henceforth in this work we shall assume that condition (7) is fulfilled. Thus in the long-time limit,  $t \rightarrow \infty$ , the memory about the initial conditions will vanish [see Eq. (A3)] as

$$\sum_{k=1}^4 H_{1k}(t)x_k(0) \approx \frac{\gamma(\omega^2 + \gamma\nu^\alpha + \nu^2)x_1(0)}{\Gamma(1-\alpha)[\omega^2(\omega^2 + \gamma\nu^\alpha + \nu^2) - a^2]t^\alpha} + O(t^{-(1+\alpha)}), \quad (8)$$

and the average oscillator displacement  $\langle X(t) \rangle$  is given by

$$\langle X \rangle_{as} \equiv \langle X \rangle|_{t \rightarrow \infty} = A_0 \int_0^t H_{12}(t-t') \cos(\Omega t') dt'. \quad (9)$$

Let us now consider, in brief, the physical meaning of inequality (7). Equation (1) can be considered as one-dimensional motion in the dichotomically switching potential profile

$$U(X, t) = -[\omega^2 + Z(t)] \frac{X^2}{2}.$$

If the noise amplitude  $a < \omega^2$ , then both potential profiles,  $U_\pm(x) = -(\omega^2 \pm a)x^2/2$ , correspond to stable dynamics with binding potentials and thus also the whole dynamics of the system (1) is stable. In the case of  $a > \omega^2$  the potential  $U_+$  corresponds to a stable state, and  $U_-$  corresponds to an unstable one (the potential is repulsive). For a very slow switching rate  $\nu \rightarrow 0$ , there is a nonzero probability that in an unstable state some trajectories tend to infinity and so the whole dynamics is unstable; thus in this case  $a_{cr}^2 = \omega^4$ . At very fast flippings,  $\nu \rightarrow \infty$ , the system (1) behaves as a stable deterministic system with the average potential  $U(X) = -\omega^2 x^2/2$  and the corresponding value of critical noise amplitude tends to infinity. In the intermediate region of the switching rate there exists a finite threshold value of the noise amplitude  $a_{cr}$ , which grows by increasing  $\nu$ , and above which the dynamics of the whole system is unstable. So, in the case of  $\omega^4 < a^2 < \omega^2(\omega^2 + \nu^2 + \gamma\nu^\alpha)$  the stability criterion (7) can be interpreted as a particular realization of the phenomenon of noise-induced stability [40] for the average oscillator displacement in model (1). Note that the above scenario is oversimplified at intermediate values of  $\nu$ , where energetic instability of higher moments (which can appear as a stochastic counterpart of the deterministic parametric reso-

nance) is possible [18]. Let us mention that in this work all results, conclusions, and figures [except for some minor details in Figs. 6(b) and 6(d)] are true also in the case of  $a^2 < \omega^4$ , i.e., if both potential profiles  $U_\pm(x) = -(\omega^2 \pm a)x^2/2$  correspond to stable dynamics, which can be relevant for large classes of biological and physical model systems, e.g., see [8,12,21,35,40,41]. Finally, we note that the physical arguments to investigate the model (1), which describes oscillator dynamics in a viscoelastic environment, are mainly the same as for the ordinary oscillator with fluctuating frequency in a normal viscous environment [12,21]. Particularly, in view of the recent experiments on protein conformational dynamics and associated theoretical models [26,32], consideration of influence of an external environmental noise in the context of such models could be useful.

### B. Complex susceptibility

From Eq. (9) it follows that the complex susceptibility  $\chi(\Omega)$  of the dynamical system (1) is given by

$$\chi(\Omega) = \chi'(\Omega) + i\chi''(\Omega) = \hat{H}_{12}(-i\Omega), \quad (10)$$

where  $\chi'(\Omega)$  and  $\chi''(\Omega)$  are the real and the imaginary parts of the susceptibility, respectively, while

$$\hat{H}_{12}(-i\Omega) = \int_0^\infty e^{i\Omega t} H_{12}(t) dt.$$

Equation (9) can be written by means of the complex susceptibility as [42]

$$\langle X \rangle_{as} = A \cos[\Omega t + \varphi], \quad (11)$$

with the output amplitude

$$A = A_0 |\chi|, \quad (12)$$

and the phase shift

$$\varphi = \arctan\left(-\frac{\chi''}{\chi'}\right). \quad (13)$$

Using Eqs. (10) and (A2) we obtain for  $A$  and  $\varphi$  that

$$A^2 = A_0^2 \frac{(f_1^2 + f_3^2)}{\left[ f_1 f_2 - \gamma \Omega^\alpha f_3 \sin\left(\frac{\pi\alpha}{2}\right) - a^2 \right]^2 + \left[ f_2 f_3 + \gamma \Omega^\alpha f_1 \sin\left(\frac{\pi\alpha}{2}\right) \right]^2}, \quad (14)$$

and

$$\varphi = \arctan\left[ \frac{a^2 f_3 + \gamma \Omega^\alpha (f_1^2 + f_3^2) \sin\left(\frac{\pi\alpha}{2}\right)}{a^2 f_1 - f_2 (f_1^2 + f_3^2)} \right], \quad (15)$$

where

$$f_1 := \omega^2 + \nu^2 - \Omega^2 + \gamma(\nu^2 + \Omega^2)^{\alpha/2} \cos\left[\alpha \arctan\left(\frac{\Omega}{\nu}\right)\right],$$

$$f_2 := \omega^2 - \Omega^2 + \gamma \Omega^\alpha \cos\left(\frac{\pi\alpha}{2}\right),$$

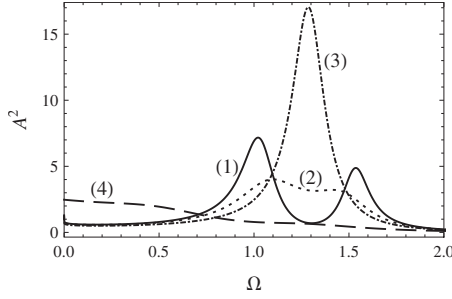


FIG. 1. The amplitude  $A$  of the mean value of the oscillator displacement  $\langle X(t) \rangle$  vs the driving frequency  $\Omega$  at  $\gamma=0.7$ ,  $A_0=\omega=1$ , and  $a^2=0.4$ . (1) Solid line:  $\alpha=0.1$  and  $\nu=0.1$ ; (2) dotted line:  $\alpha=0.1$  and  $\nu=0.3$ ; (3) dashed-dotted line:  $\alpha=0.9$  and  $\nu=1.0$ ; (4) dashed line:  $\alpha=0.9$  and  $\nu=0.1$ .

$$f_3 := 2\Omega\nu + \gamma(\nu^2 + \Omega^2)^{\alpha/2} \sin\left[\alpha \arctan\left(\frac{\Omega}{\nu}\right)\right]. \quad (16)$$

The analytical expressions (14)–(16) belong to the main results of this work. They fully determine the behavior of the average oscillator displacement in response to system parameters in the long-time limit. Also the real and the imaginary parts of the susceptibility are experimentally measured quantities for many systems [28,30] and so it is interesting to explore their behavior for system (1). The exact formulas for  $\chi'$  and  $\chi''$  are given in the Appendix by Eqs. (A4) and (A5). Here we also emphasize that for all figures throughout this work we use a dimensionless formulation of the dynamics with a scaling of the following form:

$$\tilde{\gamma} = \frac{\gamma}{\omega^{2-\alpha}}, \quad \tilde{t} = \omega t, \quad \tilde{a} = \frac{a}{\omega^2}, \quad \tilde{\nu} = \frac{\nu}{\omega}, \quad \tilde{\Omega} = \frac{\Omega}{\omega}, \quad \tilde{X} = \frac{X\omega^2}{A_0}, \quad (17)$$

i.e.,  $\tilde{\omega}=1$ ,  $\tilde{A}_0=1$ .

### III. RESULTS

#### A. Bona fide resonance

By the use of Eq. (14) we can now explicitly obtain the behavior of  $A(\Omega)$  for any combination of the system parameters  $\alpha$ ,  $\gamma$ ,  $\nu$ ,  $a$ , and  $\omega^2$ . For a conventional deterministic oscillator with  $\alpha=1$  and  $a=0$ , there is resonance if the condition  $\omega > \gamma/\sqrt{2}$  is satisfied. If this condition is not satisfied,  $A(\Omega)$  is a monotonically decreasing function of  $\Omega$ . In the case of model (1) the picture of the resonance behavior of  $A(\Omega)$  is quite different. When investigating by Eq. (14) the dependence of  $A$  on the frequency  $\Omega$ , three different types of graphs emerge for  $A(\Omega)$ . In Fig. 1 these three types are represented as depending on the parameters  $\alpha$  and  $\nu$ . In the resonance regime [curves (1)–(3) in Fig. 1], for small values of the noise switching rate  $\nu$  the positions of the resonance peaks for  $\langle X \rangle$  reproduce quite exactly the two-level structure of the multiplicative noise  $Z(t)$ . These two resonance peaks occur at the frequencies  $\Omega_{1,2} \approx \sqrt{\omega^2 + \gamma \pm a}$  if  $\alpha$  is small. By increasing the switching rate  $\nu$  the positions of both peaks shift to  $\Omega \approx \sqrt{\omega^2 + \gamma}$ , where three extrema merge [cf. curve

(2) in Fig. 1]. Such behavior of  $A(\Omega)$  is a simple consequence of the circumstance that by increasing the switching rate, the dynamical behavior of the system (1) tends to the dynamics of the corresponding deterministic system with the average potential  $U(x) = -\omega^2 x^2/2$ . If the driving frequency  $\Omega$  tends to zero, the square of the amplitude  $A$  is given by

$$A_{|\Omega=0}^2 = A_0^2 \frac{(\omega^2 + \nu^2 + \gamma\nu^\alpha)^2}{[\omega^2(\omega^2 + \nu^2 + \gamma\nu^\alpha) - a^2]^2}. \quad (18)$$

It can be seen that  $A_{|\Omega=0}^2$  tends to infinity as the noise amplitude  $a^2$  approaches the critical value  $a_{cr}^2 = \omega^2(\omega^2 + \nu^2 + \gamma\nu^\alpha)$ , i.e.,  $A_{|\Omega=0}^2$  diverges at the boundary of the stability region [see Eq. (7)]. Similarly to the case of a deterministic fractional oscillator, there exists a critical exponent  $\alpha_1$  that does not depend on other system parameters and satisfies the relation (see also [24]):

$$(\alpha_1 + 2)^2 \cos^2\left(\frac{\pi\alpha_1}{2}\right) - 8\alpha_1 = 0. \quad (19)$$

For any  $\alpha < \alpha_1 \approx 0.441$  there always exist specific frequencies  $\Omega_r$  (which depend on other system parameters) for which the system displays resonance. So the nonresonance behavior of  $A(\Omega)$  is possible only if  $\alpha > \alpha_1$  (see also Fig. 2).

Figure 2 shows phase diagrams in the  $\gamma$ – $\alpha$  plane for three values of the noise switching rate  $\nu$  at  $a^2=0.6$ . The shaded regions in the figure correspond to those regions of the parameters  $\alpha$  and  $\gamma$ , where resonance versus  $\Omega$  is possible. Two phases can be discerned in the resonance domain: the light gray region, where one resonance peak appears, and the dark gray region, where a double-peak phenomenon is observed. As the noise switching rate increases, the dashed line in Fig. 2 monotonically shifts down and disappears at a critical value of the switching rate  $\nu_c(a^2)$  which depends on the noise amplitude. Hence in the case of  $\nu > \nu_c(a^2)$  the phenomenon of double resonance is not possible. The borders of the different phases and the critical noise switching rate  $\nu_c(a^2)$  can be found from the equations

$$\frac{d}{d\Omega} A^2(\Omega) = \frac{d^2}{d\Omega^2} A^2(\Omega) = 0, \quad (20)$$

by numerical calculations. It is remarkable that the critical parameter  $\nu_c(a^2)$  increases monotonically from zero to  $\nu_{cr} \approx 0.614\omega$  when the parameter  $a^2 \in (0, \omega^4)$  increases. When the memory exponent  $\alpha$  tends to  $\alpha_1$ , the boundary between the resonance and nonresonance phases tends to infinity. Note that one of the physical explanations for the different dynamics of system (1) in the regions  $\alpha > \alpha_1$  and  $\alpha < \alpha_1$  is based on the cage effect. An excellent explanation of this effect for a deterministic fractional oscillator (without noise) is provided in [24]. According to Ref. [24], the critical memory exponent  $\alpha_1$  marks a nonsmooth transition between normal friction ( $\alpha \rightarrow 1$ ) and elastic friction ( $\alpha \rightarrow 0$ ). For small  $\alpha$  the friction force induced by the medium is not just slowing down the particle but also causing the particle to develop a rattling motion.

To see this for the stochastic oscillator (1), consider Eq. (14) in the case of adiabatic noise ( $\nu \rightarrow 0$ ). In this limit we obtain

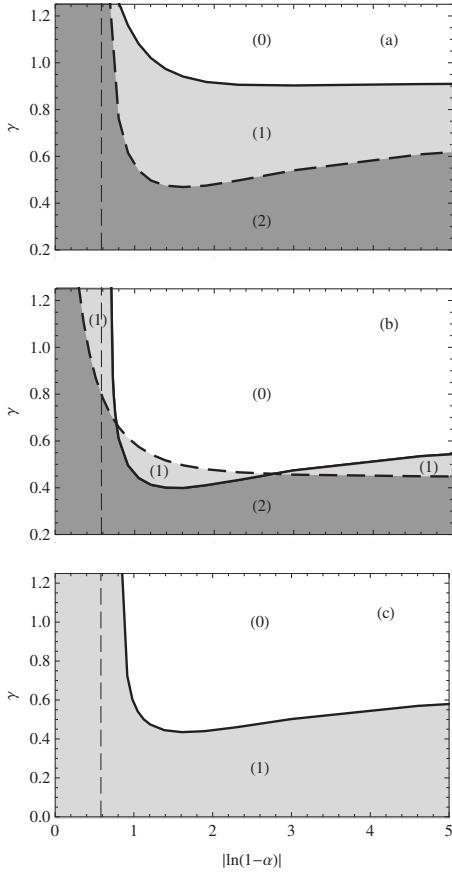


FIG. 2. A semilogarithmic plot of the phase diagram in the  $\gamma - \alpha$  plane for the existence of a resonance of  $A$  vs the driving frequency  $\Omega$  at  $A_0 = \omega = 1$ , and  $a^2 = 0.6$ . In the unshaded region (0) the resonance is impossible. The light gray region (1) corresponds to the domain where the resonance has one peak. In the dark gray region (2) a multiresonance with two peaks occurs. The thin dashed line depicts the position of the critical memory exponent  $\alpha = \alpha_1 \approx 0.441$ . The critical value of the switching rate  $\nu_{cr}(0.6) \approx 0.494$ . Panels: (a)  $\nu = 0$ , (b)  $\nu = 0.25$ , and (c)  $\nu = 0.5$ .

$$A^2 = A_0^2 \frac{(\omega_{ef}^2 - \Omega^2)^2 + \gamma_{ef}^2 \Omega^2}{[(\omega_{ef}^2 - a - \Omega^2)^2 + \gamma_{ef}^2 \Omega^2][(\omega_{ef}^2 + a - \Omega^2)^2 + \gamma_{ef}^2 \Omega^2]}, \quad (21)$$

where

$$\omega_{ef}^2 = \omega^2 + \gamma \Omega^\alpha \cos\left(\frac{\alpha\pi}{2}\right),$$

$$\gamma_{ef} = \gamma \Omega^{\alpha-1} \sin\left(\frac{\alpha\pi}{2}\right). \quad (22)$$

Formula (21) is exactly the same as can be derived from the results of [18] for an ordinary stochastic oscillator (without memory,  $\alpha = 1$ ) if we replace the eigenfrequency  $\omega$  and the friction coefficient  $\gamma$  with the corresponding effective quantities  $\omega_{ef}$  and  $\gamma_{ef}$ . Thus, our model (with memory) is equivalent to a stochastic oscillator without memory, but with the effective parameters (22). From Eqs. (22) it can easily be seen that by decreasing  $\alpha$  the effective eigenfre-

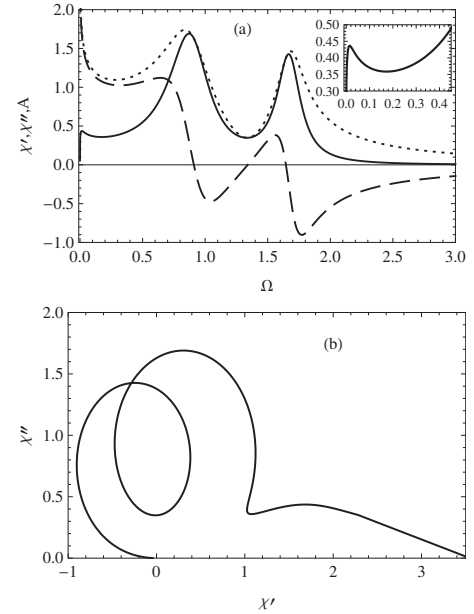


FIG. 3. Multiresonance of the response of the stochastic oscillator (1) to the driving frequency  $\Omega$ . Parameter values:  $A_0 = \omega = 1$ ,  $\alpha = 0.25$ ,  $\nu = 0.01$ ,  $\gamma = 0.8$ , and  $a^2 = 0.9$ . Panel (a): solid line: the imaginary part  $\chi''(\Omega)$  of the complex susceptibility; dashed line: the real part  $\chi'(\Omega)$  of the complex susceptibility; dotted line: the response function  $A(\Omega)$ . The inset depicts the behavior of  $\chi''$  vs  $\Omega$  at small values of the driving frequency  $\Omega$ . Panel (b): the Cole-Cole plot of  $\chi''$  as a function of  $\chi'$ . The system parameters are the same as in panel (a).

quency increases and the effective friction coefficient decreases, thus demonstrating the increasing role of elastic friction.

The existence of the cage effect for small enough  $\alpha$  is observed not only for the response function  $A$  but also for other quantities. In Fig. 3 we plot the dependencies of the imaginary and real parts of the susceptibility at a parameter regime with  $\alpha = 0.25$  on the driving frequency  $\Omega$ . An interesting peculiarity of Fig. 3(a) is that there is not only one peak present for the loss  $\chi''(\Omega)$  as is expected for a deterministic oscillator without memory, but instead we observe a three-peak phenomenon. Note that the double-peak phenomenon of the loss vs  $\Omega$  for supercooled liquids and protein solutions is a well-known phenomenon and usually treated by means of mode-coupling theory [28,43,44].

A Cole-Cole plot of complex susceptibility, presented in Fig. 3(b), shows that for this value of  $\alpha$  we have three effective characteristic frequencies in the system: the two higher frequencies correspond to the oscillating processes by the noise phases  $z = a$  and  $z = -a$  [the right side of panel (b)], while the lower one is responsible for the monotonic decay (the left side). For the deterministic fractional oscillator a corresponding interpretation of a Cole-Cole plot and a connection with a Debye model and with a Van Vleck-Weisskopf-Fröhlich type of behavior [42] have been previously considered in [24].

## B. Friction-induced resonance

The main purpose of this section is to demonstrate that a resonance-like phenomenon is manifested in the dependence

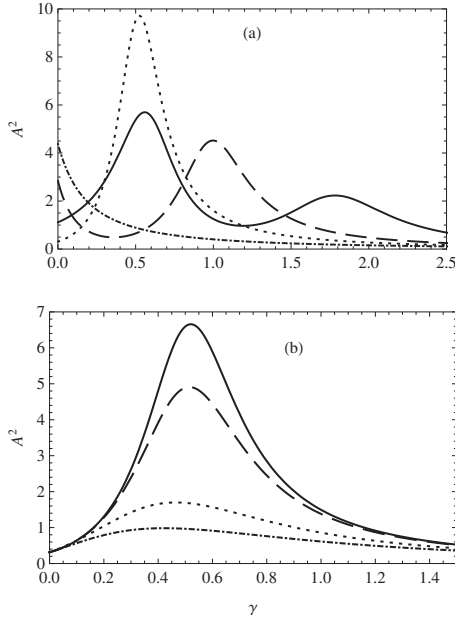


FIG. 4. Dependence of the response function  $A$  on the friction coefficient  $\gamma$  at  $A_0 = \omega = 1$ . Panel (a) depicts the resonancelike behavior of the function  $A^2(\gamma)$  at various values of the driving frequency  $\Omega$ . Other parameter values:  $\nu = 0.1$ ,  $\alpha = 0.1$ , and  $a^2 = 0.4$ . Solid line:  $\Omega = 1.5$ ; dashed line:  $\Omega = 1.18$ ; dotted line:  $\Omega = 0.95$ ; dashed-dotted line:  $\Omega = 0.3$ . Panel (b):  $A^2$  vs  $\gamma$  at different values of the memory exponent  $\alpha$ . Other parameter values:  $\nu = 0.1$ ,  $a^2 = 0.4$ , and  $\Omega = 0.95$ . Solid line:  $\alpha = 0.15$ ; dashed line:  $\alpha = 0.2$ ; dotted line:  $\alpha = 0.5$ ; dashed-dotted line:  $\alpha = 0.9$ . Note that the maximal value of  $A^2$  increases as the memory exponent  $\alpha$  decreases.

of the response  $A(\gamma)$  for the oscillator (1) upon the friction coefficient  $\gamma$ . This result is somewhat surprising because, in the corresponding deterministic models ( $\alpha = 1$ , noise absent), the amplitude of the output oscillations is well known to be monotonically decreasing when  $\gamma$  increases. In Fig. 4 several graphs depict the behavior of  $A$  versus  $\gamma$  for different representative values of other system parameters. These graphs show a typical resonancelike behavior of  $A(\gamma)$ . As a rule, the maximal value of  $A$  increases as the driving frequency  $\Omega$  decreases, while the positions of the maxima are monotonically shifted to higher  $\gamma$  as  $\Omega$  rises [see Fig. 4(a)]. Moreover, for some values of the system parameters a multiresonance with two maxima appears. Although the dependence of  $A$  on the system parameters is generally very complicated [see Eqs. (14) and (16)] and thus simple analytical conditions for the appearance of a resonance behavior of  $A$  versus  $\gamma$  are not available, it is possible to find them for some particular cases. In particular, for the case of the fast noise limit ( $\nu \rightarrow \infty$ ) we obtain that the necessary and sufficient conditions for the appearance of friction-induced resonance are

$$\alpha < 1, \quad \Omega > \omega. \quad (23)$$

The corresponding position of the maximum is determined by

$$\gamma_m = \frac{1}{\Omega^\alpha} (\Omega^2 - \omega^2) \cos\left(\frac{\alpha\pi}{2}\right). \quad (24)$$

This result is in accordance with the physical intuition that at the fast-noise limit, i.e., at very high frequencies of colored fluctuations the system is under the influence of the average eigenfrequency,  $\langle \omega^2 + Z(t) \rangle = \omega^2$ , and thus the system behaves as a deterministic fractional oscillator (without noise). Evidently, in this case the friction-induced resonance is a memory effect, because in the system without memory ( $\alpha = 1$ ) the phenomenon is absent.

At the long-correlation-time limit ( $\nu = 0$ ) we analyze the behavior of  $A$  vs  $\gamma$  for the strong memory ( $\alpha \rightarrow 0$ ) and low memory ( $\alpha \rightarrow 1$ ) regimes separately. In the case of strong memory, the following characteristic regions can be discerned for the driving frequency  $\Omega$ . (i) There is no resonance if  $\Omega^2 < \omega^2 - a$ . (ii) In the case of  $(\omega^2 - a) < \Omega^2 < \omega^2$  there exists one resonance peak. (iii) If  $\omega^2 < \Omega^2 < \omega^2 + a$ , then the curve  $A(\gamma)$  displays two extrema: a minimum and a maximum. (iv) In the case of  $\Omega^2 > \omega^2 + a$  a multiresonance with two peaks appears.

For  $\alpha = 1$ , i.e., no memory, the qualitative behavior of the response versus  $\gamma$  is different from the case of strong memory. The resonance vs  $\gamma$  exists only if

$$\omega^2 + a\sqrt{5-2} > \Omega^2 > \omega^2 - a\sqrt{5-2}, \quad (25)$$

and

$$\gamma_m = \frac{1}{\Omega} \sqrt{a\sqrt{a^2 - 4(\omega^2 - \Omega^2)^2} - (\omega^2 - \Omega^2)^2}. \quad (26)$$

Hence, the phenomenon is possible if

$$a^2 > (2 + \sqrt{5})(\omega^2 - \Omega^2)^2. \quad (27)$$

This result is in accordance with the results of Ref. [22], where friction-induced resonance for an ordinary oscillator with fluctuating frequency was previously reported. Thus, for intermediate values of  $\alpha$ ,  $0 < \alpha < 1$ , friction-induced resonance forms as a result of a nonlinear interplay between memory and colored noise generated effects. An illustration of the last mentioned claim is the formula

$$\gamma_m = \frac{a}{\omega^\alpha}, \quad (28)$$

which determines the position of the resonance peak in the case of  $\nu = 0$  and  $\Omega = \omega$ . The corresponding maximal value of  $A(\gamma)$  reads as

$$A_{\max}^2(\gamma) = \frac{A_0^2}{2a^2[1 - \cos(\pi\alpha)]}. \quad (29)$$

Evidently, the maximum of  $A$  increases rapidly as the noise amplitude  $a$  decreases or as the memory exponent  $\alpha$  tends to zero.

In conclusion, we emphasize that, as indicated by the results of this section, the formation of the multiresonance versus  $\gamma$  can be explained as a nonlinear interplay of two different resonance effects: one caused by multiplicative colored noise and another which is due to memory effects.

### C. Stochastic resonance

Our next task is to examine the dependence of the response  $A$  on the noise amplitude  $a$ . In Fig. 5 we depict the

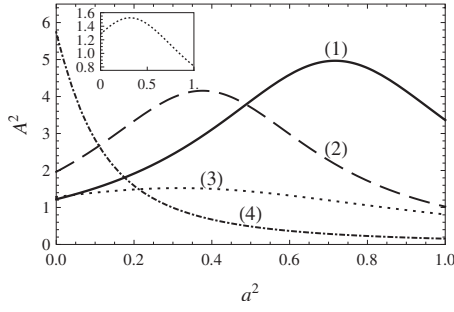


FIG. 5. SR for the response function  $A$  versus the noise amplitude  $a$  at various values of the friction coefficient  $\gamma$ . Other parameter values:  $A_0 = \omega = 1$ ,  $\nu = 0.1$ ,  $\alpha = 0.1$ , and  $\Omega = 1.8$ . (1) Solid line:  $\gamma = 1.3$ ; (2) dashed line:  $\gamma = 1.5$ ; (3) dotted line:  $\gamma = 2.85$ ; (4) dashed-dotted line:  $\gamma = 2.3$ . Note that in the case of curve (4),  $\gamma = 2.3$ , the phenomenon of stochastic resonance is absent. The inset emphasizes the nonmonotonic behavior of the curve (3).

behavior of  $A(a)$  for various values of the system parameters. As is shown in Fig. 5, curves (1)–(3) exhibit a resonancelike maximum at some values of  $a$ , i.e., a typical SR phenomenon appears at increase in  $a$  [18]. The existence of such an SR effect depends strongly on other system parameters. From Eq. (14) one can easily find the necessary and sufficient conditions for the emergence of SR due to noise amplitude variations. Namely, nonmonotonic behavior of  $A(a)$  appears in the stability region,  $0 < a < a_{cr}$  [see Eq. (7)], for the parameter regime where the following inequalities hold:

$$\gamma \Omega^\alpha f_3 \sin\left(\frac{\alpha\pi}{2}\right) < f_1 f_2 < \gamma \Omega^\alpha f_3 \sin\left(\frac{\alpha\pi}{2}\right) + a_{cr}^2. \quad (30)$$

In this case the response  $A(a)$  reaches the maximum at

$$a^2 = a_m^2 = f_1 f_2 - \gamma \Omega^\alpha f_3 \sin\left(\frac{\alpha\pi}{2}\right) < a_{cr}^2. \quad (31)$$

For example, at  $\nu = 0$  and  $\Omega = \omega$  we obtain

$$a_m^2 = \gamma^2 \omega^{2\alpha} \cos(\alpha\pi), \quad \alpha < 0.5. \quad (32)$$

In Fig. 6 the conditions (30) are illustrated in the parameter space  $(\gamma, \alpha)$  with four panels. The dark gray shaded regions in the figure correspond to those regions of the parameters  $\gamma$  and  $\alpha$ , where SR versus  $a$  is possible. Note that in the light gray regions the response  $A(a)$  formally also exhibits a resonancelike maximum, but in those regions the first moment  $\langle X(t) \rangle$  is unstable at the resonance regime and that renders formula (14) physically meaningless. The curves of the boundaries of the resonance regions are determined by the condition  $a_m^2 > 0$ , and are represented analytically in the Appendix with Eqs. (A7) and (A8). One can discern two findings. The first is the existence of a critical  $\alpha_c$ , which depends only on the ratio of the driving frequency  $\Omega$  to the noise switching rate  $\nu$ , and is given by Eq. (A9),

$$\alpha_c = \frac{\pi}{\pi + 2 \arctan(\Omega/\nu)}. \quad (33)$$

Particularly, in the adiabatic case ( $\nu \rightarrow 0$ ) the critical exponent  $\alpha_c$  is 0.5 and in the fast-noise limit ( $\nu \rightarrow \infty$ )  $\alpha_c$  tends

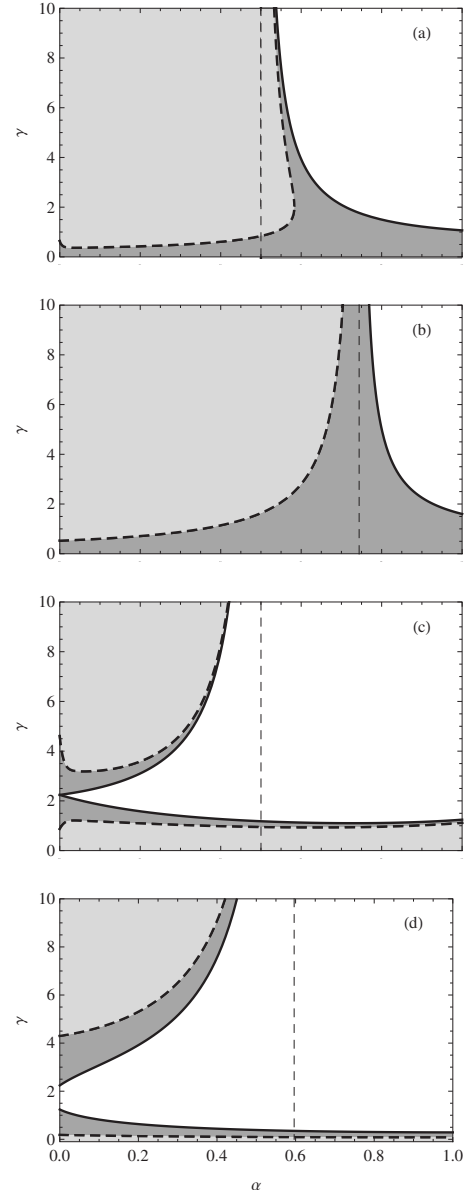


FIG. 6. A plot of the phase diagrams for SR in the  $\gamma$ – $\alpha$  plane at  $A_0 = \omega = 1$ . In the unshaded region the resonance of  $A$  versus the noise amplitude  $a$  is impossible. In the light gray region the function  $A(a)$  exhibits a maximum at  $a_m > a_{cr}$  [see Eq. (7)], i.e., at  $a_m$  the first moment of the oscillator displacement  $\langle X(t) \rangle$  is unstable. In the dark gray domain a stochastic resonance for  $A$  vs  $a$  occurs (in the stability region). The thin dashed line depicts the position of the critical memory exponent  $\alpha_c$ , [Eq. (33)]. Panel (a):  $\nu = 0$ ,  $\Omega = 0.6$ ; panel (b):  $\nu = 1.0$ ,  $\Omega = 0.6$ ; panel (c):  $\nu = 0$ ,  $\Omega = 1.8$ ; panel (d):  $\nu = 1.0$ ,  $\Omega = 1.8$ .

to 1. It is seen that the critical exponent  $\alpha_c$  marks a sharp transition in the behavior of systems with fractional dynamics. At  $\alpha_c$ , one of the boundaries  $\gamma(\alpha)$  between the resonance and nonresonance regions tends to infinity. The second finding is that depending on the driving frequency  $\Omega$ , three different cases can be discerned. (i) For  $\Omega^2 < \omega^2$ , the resonance vs  $a$  appears in the stability region for all values of  $\gamma$  when  $\alpha < \alpha_c$ , but if  $\alpha > \alpha_c$ , there is an upper border  $\gamma(\alpha)$  above which the resonance is absent [Figs. 6(a) and 6(b)]. (ii) In the

case of  $\omega^2 < \Omega^2 < \omega^2 + \nu^2$ , for  $\alpha < \alpha_c$ , the resonance exists only if  $\gamma > \Omega^2 - \omega^2$ ; in the region  $\alpha > \alpha_c$  the resonance is absent. (iii) At the driving frequency regime  $\Omega^2 > \omega^2 + \nu^2$ , if  $\alpha < \alpha_c$ , the interesting peculiarity of the diagram is that there are two disconnected regions [the shaded areas in Figs. 6(c) and 6(d)] where the resonance can appear. Thus, in this case increasing (decreasing) values of the friction parameter  $\gamma$  induce reentrant transitions between different dynamical regimes of the oscillator. Namely, an increase in  $\gamma$  can induce transitions from a regime where SR versus  $a$  is possible to the regime where SR is absent, but SR appears again through a reentrant transition at higher values of  $\gamma$ . An important observation here is that the region where the resonance is not possible grows as the noise switching rate  $\nu$  increases. This tendency is in accordance with the fact that at high values of the noise switching rate the system (1) behaves as a deterministic fractional oscillator (without noise). At  $\alpha = 0$  the resonance is possible if  $\gamma > \Omega^2 - \omega^2$  or if  $\gamma < \Omega^2 - \omega^2 - \nu^2$ . For  $\alpha > \alpha_c$  the resonance appears only for relatively small values of  $\gamma$ . In the case of  $\alpha = 1$  the upper value of  $\gamma$  is given by

$$\gamma = \frac{1}{2\Omega^2} \left[ \nu(\omega^2 - 3\Omega^2) + \sqrt{4\Omega^4\nu^2 + (\omega^2 - \Omega^2)^2(4\Omega^2 + \nu^2)} \right]. \quad (34)$$

These results are highly unexpected for SR, but agree with the description of the friction force for small  $\alpha$  as an elastic force due to the cage effect. To clarify the last statement, let us take a closer look at the adiabatic limit,  $\nu \rightarrow 0$ . From Eqs. (21) and (22) we obtain, that SR versus  $a$  is possible if the effective friction coefficient  $\gamma_{ef}$  is sufficiently small in comparison with the difference between the driving frequency  $\Omega$  and the effective eigenfrequency  $\omega_{ef}$ , i.e.,

$$\gamma_{ef} < \frac{|\omega_{ef}^2 - \Omega^2|}{\Omega}. \quad (35)$$

As because of the cage effect, by decreasing the memory exponent  $\alpha$  the effective friction coefficient  $\gamma_{ef}$  decreases and  $\omega_{ef}$  increases [cf. Eq. (22)], the difference between the regimes  $\Omega > \omega$  and  $\Omega < \omega$  is not surprising. Namely, in the case of  $\Omega < \omega$  the right side of the inequality (35) increases monotonically as  $\alpha$  decreases, but if  $\Omega > \omega$ , the dependence of  $|\omega_{ef}^2 - \Omega^2|$  on  $\alpha$  is either monotonically decreasing or non-monotonic. It is remarkable that in the adiabatic case, the borders  $\gamma_{\pm}(\alpha)$  of the SR domains are given by a relatively simple formula [cf. also Figs. 6(a) and 6(c), and Eqs. (A7) and (A8)]

$$\gamma_{\pm}(\alpha) = \frac{\Omega^2 - \omega^2}{\Omega^{\alpha} \left[ \cos\left(\frac{\pi\alpha}{2}\right) \pm \sin\left(\frac{\pi\alpha}{2}\right) \right]}, \quad \gamma \geq 0. \quad (36)$$

Note a singular behavior of  $\gamma_{-}(\alpha)$  at  $\alpha = \alpha_c = 0.5$ .

Finally, the phenomenon of SR is not restricted to non-monotonic dependence of  $A$  on the noise amplitude  $a$ . Figure 7 depicts the behavior of the response  $A$  versus the noise switching rate  $\nu$  for different values of the friction coefficient  $\gamma$ . In this figure, one observes the resonance versus  $\nu$ , which apparently gets more and more pronounced as the friction

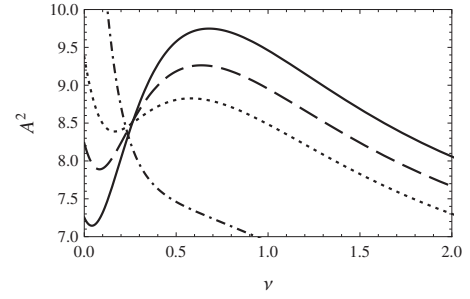


FIG. 7. SR for  $A^2$  versus the noise switching rate  $\nu$ , computed from Eq. (14) at various values of the friction coefficient  $\gamma$ . Other parameter values:  $A_0 = \omega = 1$ ,  $a^2 = 0.3$ ,  $\alpha = 0.3$ , and  $\Omega = 0.8$ . Solid line:  $\gamma = 0.04$ ; dashed line:  $\gamma = 0.05$ ; dotted line:  $\gamma = 0.06$ ; dashed-dotted line:  $\gamma = 0.1$ . Note that in the case of  $\gamma = 0.1$  the phenomenon of stochastic resonance is absent.

coefficient  $\gamma$  decreases. It is remarkable that in contrast to the case  $A$  vs  $a$ , SR vs  $\nu$  depends on the exponent  $\alpha$  very weakly: as  $\alpha$  increases from 0 to 1 only a slight deformation of the curves  $A(\nu)$  can be observed.

#### IV. CONCLUSIONS

We have studied, in the long-time regime, the response function, and the complex susceptibility of a stochastic fractional oscillator with a power-law memory kernel for the friction term. The influence of the fluctuating medium is modeled by a multiplicative dichotomous noise. The Shapiro-Logvinov formula [38] allows us to find a closed system of equations for the first-order moments and an exact expression for the complex susceptibility. A major virtue of the investigated model is that an interplay of the colored dichotomous noise, the external periodic forcing, and memory effects in a noisy, fractional oscillator can generate a rich variety of nonequilibrium cooperation phenomena. Namely, (i) multiresonance of the imaginary part of the susceptibility versus the frequency of the driving force  $\Omega$  (up to three peaks); (ii) existence of the critical memory exponent  $\alpha_1 \approx 0.441$  below which ( $\alpha < \alpha_1$ ) the resonance vs  $\Omega$  of the amplitude of the mean oscillator displacement  $\langle X(t) \rangle$  occurs for all values of the other system parameters (cf. also [24]); (iii) friction-induced multiresonance, i.e., two resonance peaks of the response function can be evoked by varying the friction coefficient; (iv) a nonmonotonic dependence of the response function on the amplitude  $a$  and the switching rate  $\nu$  of the multiplicative noise (i.e., SR); (v) the existence of a band gap for values of the friction coefficient  $\gamma$  between two regions of  $\gamma$ - $\alpha$  phase diagrams where SR vs  $a$  is possible at sufficiently small values of the memory exponent  $\alpha < \alpha_c(\Omega/\nu)$ , and the associated friction-induced reentrant transitions between different dynamical regimes of the oscillator; particularly, the minimal value of the critical exponent  $\alpha_c$  is 0.5.

We believe that the results of this paper not only supply material for theoretical investigations of fractional dynamics in stochastic systems, but also suggest some possibilities for interpreting experimental subdiffusion results in biological

applications, where the issues of memory and multiplicative colored noise can be crucial [30,35].

A further detailed study is, however, necessary especially an investigation of the behavior of second moments. It remains to be seen how the reported phenomena can be useful to experimenters in the fields of stochastic resonance, biopolymers, and transient dynamics of molecular and colloidal glasses.

### ACKNOWLEDGMENTS

The work was supported by the Estonian Science Foundation under Grant No. 7319, by the Ministry of Education and Research of Estonia under Grant No. SF0132723s06, and by the International Atomic Energy Agency under Grant No. 14797.

### APPENDIX: FORMULAS FOR THE RELAXATION FUNCTIONS

#### 1. Laplace transforms of the relaxation functions

The relaxation functions  $H_{ik}(t)$  in Eq. (5) can be obtained by means of the Laplace transformation technique.

From Eqs. (4) and (5) with the initial conditions

$$H_{ik}(0) = \delta_{ik},$$

we obtain the following system of algebraic linear equations for  $\hat{H}_{ik}(s)$ :

$$\begin{aligned} s\hat{H}_{1k} - \hat{H}_{2k} &= \delta_{1k}, \\ (s + \gamma s^{\alpha-1})\hat{H}_{2k} + \omega^2\hat{H}_{1k} + \hat{H}_{3k} &= \delta_{2k}, \\ (s + \nu)\hat{H}_{3k} - \hat{H}_{4k} &= \delta_{3k}, \\ [s + \nu + \gamma(s + \nu)^{\alpha-1}]\hat{H}_{4k} + \omega^2\hat{H}_{3k} + a^2\hat{H}_{1k} &= \delta_{4k}, \end{aligned} \quad (\text{A1})$$

where  $k=1, \dots, 4$  and  $\hat{H}_{ik}(s)$  is the Laplace transform of  $H_{ik}(t)$ , i.e.,

$$\hat{H}_{ik}(s) = \int_0^\infty e^{-st} H_{ik}(t) dt.$$

The solution of Eq. (A1) reads as

$$\begin{aligned} \hat{H}_{11}(s) &= \frac{1}{D(s)}(s + \gamma s^{\alpha-1})[\omega^2 + (s + \nu)^2 + \gamma(s + \nu)^\alpha], \\ \hat{H}_{21}(s) &= \frac{1}{D(s)}\{a^2 - \omega^2[\omega^2 + (s + \nu)^2 + \gamma(s + \nu)^\alpha]\}, \\ \hat{H}_{31}(s) &= -\frac{a^2}{D(s)}(s + \gamma s^{\alpha-1}), \\ \hat{H}_{41}(s) &= -\frac{a^2}{D(s)}(s + \nu)(s + \gamma s^{\alpha-1}), \end{aligned}$$

$$\hat{H}_{12}(s) = \frac{1}{D(s)}[\omega^2 + (s + \nu)^2 + \gamma(s + \nu)^\alpha],$$

$$\hat{H}_{22}(s) = \frac{s}{D(s)}[\omega^2 + (s + \nu)^2 + \gamma(s + \nu)^\alpha],$$

$$\hat{H}_{32}(s) = -\frac{a^2}{D(s)},$$

$$\hat{H}_{42}(s) = -\frac{a^2}{D(s)}(s + \nu),$$

$$\hat{H}_{13}(s) = -\frac{1}{D(s)}[s + \nu + \gamma(s + \nu)^{\alpha-1}],$$

$$\hat{H}_{23}(s) = -\frac{s}{D(s)}[s + \nu + \gamma(s + \nu)^{\alpha-1}],$$

$$\hat{H}_{33}(s) = \frac{1}{D(s)}[s^2 + \gamma s^\alpha + \omega^2][s + \nu + \gamma(s + \nu)^{\alpha-1}],$$

$$\hat{H}_{43}(s) = \frac{1}{D(s)}[a^2 - \omega^2(s^2 + \gamma s^\alpha + \omega^2)],$$

$$\hat{H}_{14}(s) = -\frac{1}{D(s)},$$

$$\hat{H}_{24}(s) = -\frac{s}{D(s)},$$

$$\hat{H}_{34}(s) = \frac{1}{D(s)}(s^2 + \gamma s^\alpha + \omega^2),$$

$$\hat{H}_{44}(s) = \frac{1}{D(s)}(s + \nu)(s^2 + \gamma s^\alpha + \omega^2), \quad (\text{A2})$$

where

$$D(s) = (s^2 + \gamma s^\alpha + \omega^2)[\omega^2 + (s + \nu)^2 + \gamma(s + \nu)^\alpha] - a^2.$$

#### 2. Asymptotic behavior of the relaxation functions

Now we present the behavior of the functions  $H_{1k}(t)$ ,  $k=1, \dots, 4$ , at a long-time limit ( $t \rightarrow \infty$ ). The asymptotic behavior of  $H_{1k}(t)$  is obtained from Eq. (A2) using the Tauberian theorem [45]

$$H_{11}(t) \approx \frac{\gamma b}{(\omega^2 b - a^2)\Gamma(1 - \alpha)} t^{-\alpha},$$

$$H_{12}(t) \approx \frac{\gamma \alpha b^2}{(\omega^2 b - a^2)^2 \Gamma(1 - \alpha)} t^{-(1+\alpha)},$$

$$H_{13}(t) \approx -\frac{\gamma \alpha b (\nu + \gamma \nu^{\alpha-1})}{(\omega^2 b - a^2)^2 \Gamma(1 - \alpha)} t^{-(1+\alpha)},$$

$$H_{14}(t) \approx - \frac{\gamma \alpha b}{(\omega^2 b - a^2)^2 \Gamma(1 - \alpha)} t^{-(1+\alpha)}, \quad (\text{A3})$$

where  $t \rightarrow \infty$  and  $b := \omega^2 + \nu^2 + \gamma \nu^\alpha$ . From Eq. (A3) it follows that for large  $t$  the relaxation function  $H_{1k}(t)$  decays as a power law. Note that the applicability of Eq. (A3) is possible only under the condition:  $a^2 < \omega^2 b$ , [cf. Eq. (7)].

### 3. Complex susceptibility

Here the exact formulas for the imaginary part  $\chi''$  and for the real part  $\chi'$  of the complex susceptibility will be represented. From Eqs. (10) and (A2) one can conclude that the quantities  $\chi''$  and  $\chi'$  are given by

$$\chi' = \frac{f_2(f_1^2 + f_3^2) - a^2 f_1}{\left[ f_1 f_2 - \gamma \Omega^\alpha f_3 \sin\left(\frac{\pi\alpha}{2}\right) - a^2 \right]^2 + \left[ f_2 f_3 + \gamma \Omega^\alpha f_1 \sin\left(\frac{\pi\alpha}{2}\right) \right]^2}, \quad (\text{A4})$$

and

$$\chi'' = \frac{\gamma \Omega^\alpha (f_1^2 + f_3^2) \sin\left(\frac{\pi\alpha}{2}\right) + a^2 f_3}{\left[ f_1 f_2 - \gamma \Omega^\alpha f_3 \sin\left(\frac{\pi\alpha}{2}\right) - a^2 \right]^2 + \left[ f_2 f_3 + \gamma \Omega^\alpha f_1 \sin\left(\frac{\pi\alpha}{2}\right) \right]^2}, \quad (\text{A5})$$

where the coefficients  $f_j$ ,  $j=1,2,3$ , are determined by Eq. (16).

### 4. Critical exponent $\alpha_c$

The regions in the parameter space  $(\gamma, \alpha)$  where SR versus the noise amplitude  $a$  is possible, are determined by the inequality  $a_m^2 > 0$  with Eq. (31). The boundaries  $\gamma_{1,2}(\alpha)$  of those regions are given by

$$a_m^2 = f_1 f_2 - \gamma \Omega^\alpha f_3 \sin\left(\frac{\pi\alpha}{2}\right) = 0, \quad (\text{A6})$$

where  $f_1, f_2$  and  $f_3$  are expressed in Eq. (16). From Eqs. (16) and (A6) it follows, that

$$\gamma_{1,2} = \frac{1}{2g} (-b \pm \sqrt{b^2 - 4cg}), \quad (\text{A7})$$

while

$$c = (\omega^2 - \Omega^2)(\omega^2 + \nu^2 - \Omega^2),$$

$$b = \Omega^\alpha (\omega^2 + \nu^2 - \Omega^2) \cos\left(\frac{\pi\alpha}{2}\right) - 2\nu \Omega^{\alpha+1} \sin\left(\frac{\pi\alpha}{2}\right) + (\omega^2 - \Omega^2)(\nu + \Omega^2)^{\alpha/2} \cos\left[\alpha \arctan\left(\frac{\Omega}{\nu}\right)\right],$$

$$g = \Omega^\alpha (\nu^2 + \Omega^2)^{\alpha/2} \cos\left\{\alpha \left[\arctan\left(\frac{\Omega}{\nu}\right) + \frac{\pi}{2}\right]\right\}. \quad (\text{A8})$$

It can be seen from Eqs. (A7) and (A8), that one of the boundaries  $\gamma_{1,2}(\alpha)$  tends to infinity if  $g$  tends to zero. This happens as the memory exponent  $\alpha$  tends to  $\alpha_c$ , where

$$\alpha_c = \frac{\pi}{\pi + 2 \arctan\left(\frac{\Omega}{\nu}\right)}. \quad (\text{A9})$$

Thus, we have obtained Eq. (33).

- [1] R. Benzi, A. Sutera, and A. Vulpiani, *J. Phys. A* **14**, L453 (1981).  
 [2] L. Gammaitoni, P. Hänggi, P. Jung, and F. Marchesoni, *Rev. Mod. Phys.* **70**, 223 (1998).  
 [3] V. Berdichevsky and M. Gitterman, *Phys. Rev. E* **60**, 1494 (1999).  
 [4] M. O. Magnasco, *Phys. Rev. Lett.* **71**, 1477 (1993); P. Reimann, *Phys. Rep.* **361**, 57 (2002); R. Mankin, R. Tammelo,

- and D. Martila, *Phys. Rev. E* **64**, 051114 (2001).  
 [5] J. García-Ojalvo and J. M. Sancho, *Noise in Spatially Extended Systems* (Springer-Verlag, New York, 1999).  
 [6] R. Müller, K. Lippert, A. Kühnel, and U. Behn, *Phys. Rev. E* **56**, 2658 (1997); A. A. Zaikin, J. J. García-Ojalvo, and L. Schimansky-Geier, *ibid.* **60**, R6275 (1999); S. Kim, S. H. Park, and C. S. Ryu, *Phys. Rev. Lett.* **78**, 1616 (1997).  
 [7] A. Sauga and R. Mankin, *Phys. Rev. E* **71**, 062103 (2005).

- [8] R. Mankin, T. Laas, A. Sauga, A. Ainsaar, and E. Reiter, *Phys. Rev. E* **74**, 021101 (2006); R. Mankin, T. Laas, E. Soika, and A. Ainsaar, *Eur. Phys. J. B* **59**, 259 (2007).
- [9] R. Metzler and J. Klafter, *Phys. Rep.* **339**, 1 (2000).
- [10] C. C. Bloch, *Classical and Quantum Oscillator* (Wiley, New York, 1997).
- [11] S. Chandrasekhar, *Rev. Mod. Phys.* **15**, 1 (1943).
- [12] K. Lindenberg, V. Seshadri, and B. J. West, *Phys. Rev. A* **22**, 2171 (1980).
- [13] J. I. Jiménez-Aquino, R. M. Velasco, and F. J. Uribe, *Phys. Rev. E* **77**, 051105 (2008); F. K. Abdullaev, S. A. Darmanyany, and M. R. Djumaev, *Phys. Lett. A* **141**, 423 (1989); P. S. Landa and A. A. Zaikin, *Phys. Rev. E* **54**, 3535 (1996); P. S. Landa, A. A. Zaikin, M. G. Rosenblum, and J. Kurths, *ibid.* **56**, 1465 (1997); C.-I. Um, K. H. Yeon, and T. F. George, *Phys. Rep.* **362**, 63 (2002).
- [14] M. Turelli, *Theoretical Population Biology* (Academic, New York, 1977).
- [15] N. G. van Kampen, *Stochastic Processes in Physics and Chemistry* (North-Holland, Amsterdam, 1981).
- [16] M. Bier and R. D. Astumian, *Phys. Rev. Lett.* **76**, 4277 (1996).
- [17] R. C. Bourret, U. Frisch, and A. Pouquet, *Physica (Utrecht)* **65**, 303 (1973).
- [18] R. Mankin, K. Laas, T. Laas, and E. Reiter, *Phys. Rev. E* **78**, 031120 (2008).
- [19] I. Bena, C. Van den Broeck, R. Kawai, M. Copelli, and K. Lindenberg, *Phys. Rev. E* **65**, 036611 (2002).
- [20] S. J. Fraser and R. Kapral, *Phys. Rev. A* **45**, 3412 (1992).
- [21] M. Gitterman, *Phys. Rev. E* **67**, 057103 (2003); M. Gitterman, *The Noisy Oscillator* (World Scientific, Singapore, 2005).
- [22] K. Laas, R. Mankin, and A. Rekker, *Phys. Rev. E* **79**, 051128 (2009).
- [23] Y.-R. Zhou, F. Guo, S.-Q. Jiang, and X.-F. Pang, *Chin. J. Phys. (Taipei)* **45**, 469 (2007).
- [24] S. Burov and E. Barkai, *Phys. Rev. E* **78**, 031112 (2008).
- [25] A. D. Viñales and M. A. Despósito, *Phys. Rev. E* **73**, 016111 (2006); M. A. Despósito and A. D. Viñales, *Phys. Rev. E* **77**, 031123 (2008); K. G. Wang and M. Tokuyama, *Physica A* **265**, 341 (1999); W. Götze and M. Sperl, *Phys. Rev. Lett.* **92**, 105701 (2004).
- [26] S. C. Kou and X. S. Xie, *Phys. Rev. Lett.* **93**, 180603 (2004).
- [27] E. Lutz, *Phys. Rev. E* **64**, 051106 (2001); R. Metzler and J. Klafter, *ibid.* **61**, 6308 (2000); W. T. Coffey, Yu. P. Kalmykov, and J. T. Waldron, *The Langevin Equation* (World Scientific, Singapore, 2004); N. Pottier and A. Mauger, *Physica A* **332**, 15 (2004).
- [28] W. Gotze and L. Sjögren, *Rep. Prog. Phys.* **55**, 241 (1992).
- [29] T. Carlsson, L. Sjögren, E. Mamontov, and K. Psiuk-Maksymowicz, *Phys. Rev. E* **75**, 031109 (2007).
- [30] T. G. Mason and D. A. Weitz, *Phys. Rev. Lett.* **74**, 1250 (1995); I. Golding and E. C. Cox, *ibid.* **96**, 098102 (2006); I. M. Tolić-Nørrelykke, E.-L. Munteanu, G. Thon, L. Oddershede, and K. Berg-Sørensen, *ibid.* **93**, 078102 (2004); G. Guigas, C. Kalla, and M. Weiss, *Biophys. J.* **93**, 316 (2007); D. S. Banks and C. Fradin, *ibid.* **89**, 2960 (2005).
- [31] Qing Gu, E. A. Schiff, S. Grebner, F. Wang, and R. Schwarz, *Phys. Rev. Lett.* **76**, 3196 (1996).
- [32] W. Min, G. Luo, B. J. Cherayil, S. C. Kou, and X. S. Xie, *Phys. Rev. Lett.* **94**, 198302 (2005).
- [33] S. Chaudhury, S. C. Kou, and B. J. Cherayil, *J. Phys. Chem. B* **111**, 2377 (2007).
- [34] J. D. Bao and Y. Z. Zhuo, *Phys. Rev. C* **67**, 064606 (2003).
- [35] R. D. Astumian and M. Bier, *Biophys. J.* **70**, 637 (1996).
- [36] W. Horsthemke and R. Lefever, *Noise-Induced Transitions* (Springer-Verlag, Berlin, 1984).
- [37] R. Kubo, *Rep. Prog. Phys.* **29**, 255 (1966).
- [38] V. E. Shapiro and V. M. Loginov, *Physica A* **91**, 563 (1978).
- [39] S. Kempfle, J. Schäfer, and H. Beyer, *Nonlinear Dyn.* **29**, 99 (2002).
- [40] R. A. Ibrahim, *J. Vib. Control* **12**, 1093 (2006); B. Spagnolo, A. A. Dubkov, and N. V. Agudov, *Acta Phys. Pol. B* **35**, 1419 (2004); R. Mankin, E. Soika, A. Sauga, and A. Ainsaar, *Phys. Rev. E* **77**, 051113 (2008).
- [41] P. D'Odorico, F. Laio, and L. Ridolfi, *Proc. Natl. Acad. Sci. U.S.A.* **102**, 10819 (2005).
- [42] R. Kubo, M. Toda, and N. Hashitsume, *Statistical Physics II, Nonequilibrium Statistical Mechanics* (Springer-Verlag, Berlin, 1985).
- [43] W. Götze and M. R. Mayr, *Phys. Rev. E* **61**, 587 (2000).
- [44] M. Sperl, *Phys. Rev. E* **74**, 011503 (2006).
- [45] W. Feller, *An Introduction to Probability Theory and Its Applications* (Wiley, New York, 1971), Vol. II.